Catalysis Today 225 (2014) 10–17

Contents lists available at ScienceDirect

Catalysis Today

journal homepage: www.elsevier.com/locate/cattod

Rapid degradation of toxic toluene using novel mesoporous SiO_2 doped TiO_2 nanofibers

Sihui Zhan[a,b,c,*], Yang Yang[a,b], Xichao Gao[a,b], Hongbing Yu[a,b], Shanshan Yang[a,b], Dandan Zhu[a,b], Yi Li[c,d,**]

[a] College of Environmental Science and Engineering, Nankai University, Tianjin 300071, PR China
[b] Key Laboratory of Environmental Pollution Process and Environmental Criteria, Ministry of Education, Nankai University, PR China
[c] Department of Chemistry and Biochemistry, University of Notre Dame, Notre Dame, IN 46556, United States
[d] Department of Chemistry, Tianjin University, Tianjin 300072, PR China

ARTICLE INFO

Article history:
Received 22 May 2013
Received in revised form 8 August 2013
Accepted 22 August 2013
Available online 17 September 2013

Keywords:
Toluene
Fibrous catalyst
Doped
Degradation mechanism

ABSTRACT

Toluene is a typical volatile organic compound (VOC), which is harmful to human. The novel mesoporous TiO_2 composite fibers with optimal SiO_2 content were fabricated via electrospinning the relevant gel precursor, and were characterized by XRD, SEM, TEM, TG–DTA, UV–vis, and BET surface analysis, respectively. Through photocatalytic degradation of gaseous toluene with these nanostructured fibrous catalysts, it has shown that 10% silica doped TiO_2 nanofibers displayed the highest degradation rate among a lot of titania fibers with different silica content, and whose reaction rate is two-fold enhancement than Degussa P25. What is more, it is easy to fix and recycle nanofibrous catalysts. Furthermore, the degradation pathway of cleaning toluene has been verified based on GC–MS detection.

1. Introduction

Nowadays, it is very urgent to clean toxic toluene, one most typical volatile organic compound (VOC), from indoor air, due to a good many of people are suffering from them released from construction projects, interior decorations, daily necessities, and so on [1–3].

Up to date, various approaches have been used to clean toluene successfully, such as absorption, biofiltration, condensation and catalytic processes. However, they are usually restricted in actual application because of their high cost of equipment and operations, secondary pollution and complex pretreatment processes, etc. [4–8]. The photocatalytic oxidation (PCO) process attracts huge attentions due to its superior advantages of cost-effective, environmentally friendly and higher efficiency in cleaning VOCs under ultraviolet or near-UV light source. What is more, it can be realized that VOCs could be turned into CO_2 and H_2O under ambient conditions without other harmful byproducts [9].

Titanium oxide (TiO_2) is the most famous n-type semiconductor PCO catalysts, which has been used for photocatalytic degradation of many organic pollutants, because of their remarkable advantages, such as inexpensive, biological and chemical inertness, structural stability [10,11]. However, while using pure anatase TiO_2 for cleaning toluene or other organic pollutants, the lower degradation efficiency and necessary long irradiation period greatly limit its practical applications [12–14]. Moreover, several methods have been developed to increase its photocatalytic activity, such as metal, transition metal or non-metal deposition, or coupling with a narrow band gap semiconductor [15–17]. Wang and coworkers have prepared C-doped hollow mesoporous TiO_2 microspheres, which exhibited higher photocatalytic activity for removing toluene [18]. Ge's group found that the total conversion ratio of benzaldehyde and benzoic acid could exceed 80% when using Ag element doped V_2O_5/TiO_2 as catalyst [19]. However, all the above catalysts all face the difficulties about how to fix or recycle used catalysts.

Recently, one-dimensional nanostructured fibers can found to be prepared through electrospinning their relevant gel precursors, which aroused people's widespread interests due to their flexibility cloths, low cost and high yield. Therefore, electrospun fibers have been widely used to clean pollutants in air or water environment

* Corresponding author at: College of Environmental Science and Engineering, Nankai University, Tianjin 300071, PR China. Tel.: +86 22 23502756; fax: +86 22 23502756.
** Corresponding author at: Department of Chemistry, Tianjin University, Tianjin 300072, PR China. Tel.: +86 22 27403475; fax: +86 22 27403475.
E-mail addresses: sihuizhan@nankai.edu.cn, sihuizhan@gmail.com (S. Zhan), liyi@tju.edu.cn (Y. Li).

0920-5861/$ – see front matter.
http://dx.doi.org/10.1016/j.cattod.2013.08.018

[20–23]. While using electrospun nanofibrous catalysts to remove organic pollutants, several practical drawbacks of nanoparticles can be overcome, because it is very easy to fix and recycle these fibrous catalysts.

In this paper, mesoporous TiO_2 nanostructured fibers with different SiO_2 doped ratio has been firstly prepared using electrospinning technology combined with sol–gel methods. Their photocatalytic performances were verified through degradating gaseous toluene under UV light, showing that 10% is the optimal SiO_2 doped ratio. Moreover, many process parameters affecting ultima degradation efficiency have also been determined, such as sintered temperature, ambient humidity, irradiation time and initial concentration of toluene. And the degradation mechanism of gaseous toluene has been proposed through detecting intermediate products using gas chromatography and mass spectrometry (GC–MS). On the other side, it is easy to fix and recover the long mesoporous SiO_2 doped TiO_2 fibers while cleaning toluene, which is favor of extensive application in the near future.

2. Experimental

2.1. Sample preparation

Hydrochloric acid (37.5 wt%), tetraethoxysilane (TEOS), titanium n-butyloxide ($Ti(OC_4H_9{}^n)_4$, TBOT), Pluronic P123 (Sigma–Aldrich) and ethanol (>99.7%) were obtained from Sinopharm Chemical Reagent Co., Ltd. without further purification. In a typical procedure, 0.37 mmol P123 was dissolved in 5.0 mL absolute ethanol, and 10.0 mmol $Ti(OC_4H_9{}^n)_4$ was added with strongly stirring. Different amounts of TEOS were added into the above solution, according to the Si/Ti molar ratio of 1:100, 5:100, 10:100, 15:100, and 20:100, which were marked as 1%, 5%, 10%, 15% and 20%, separately. After being dissolved completely, 0.5 mL of concentrated HCl was added to adjust pH value of the solution for avoiding hydrolysis of alkoxide. After being strongly stirred for 30 min at room temperature, the solution was then aged at 50 °C, until to get a transparent spinnable precursor sol.

While the spinnable precursor sol came into being, it was transferred into a plastic syringer, which was pressurized with a micro feed pump (Cole-Parmer 74900-05, USA). A piece of self-made stainless steel board was put under the bottom to collect the electrosun gel fibers at room temperature, and a metallic hollow needle was connected to a high-voltage supply (DW-P503-4ACCD, Tianjin, China). The applied voltage was 15 kV, the distance between the spinneret and the collector was 15 cm, and gel fibers were left in air for 6 h to allow these gel fibers to hydrolyze completely, then the xerogel fibers were obtained. In order to remove organics completely, the obtained xerogel fibers were first sintered at 130 °C for 8 h, then increased to a target temperature at a heating rate of 1 °C min^{-1}. After being cooled to room temperature naturally, mesoporous SiO_2 doped TiO_2 nanostructured fibers with different Si/Ti molar ratio were obtained successfully.

2.2. Characterization

The structure and morphology of nanofibers were observed using a high-resolution transmission electron microscopy (HRTEM, Tecnai G2F20) and field-emission scanning electron microscopy (FESEM, HITACHI S-4800). The X-ray diffraction (XRD) patterns of fibers were recorded via an X-ray diffractometer (Rigaku D/Max 2200PC) with a graphite monochrometer and Cu Kα radiation (λ = 0.15418 nm) in the range of 20–80° at room temperature, with the voltage and electric current being fixed at 28 kV and 20 mA. The Fourier transform infrared (FTIR) spectroscopy spectra were recorded on a Nicolet 5DX-FTIR spectrometer using KBr pellet method in the range of 400–4000 cm^{-1}. Thermal gravimetric analysis (TGA) was employed under an air flow of 20 mL min^{-1} and heating rate of 20 °C min^{-1} using a thermal analyzer (NETZSCH TG 209). The specific surface area, total pore volume, and average pore size were calculated using the surface area and pore-size analyzer (Quantachrome Autosorb iQ-MP, USA) at 77 K with samples degassed under vacuum at 273 K prior to each test. X-ray photoelectron spectroscopy (XPS) spectra were collected on a Kratos Axis Ultra DLD multi-technique X-ray photoelectron spectrometer (UK) using a monochromatic Al Kα X-ray source ($h\nu$ = 1486.6 eV). All XPS spectra were recorded using an aperture slot of 300 × 700 microns, survey spectra were recorded with a pass energy of 160 eV, and high resolution spectra with a pass energy of 40 eV.

2.3. Photocatalytic test

The photocatalytic activities of the mesoporous SiO_2 doped TiO_2 fibers with different SiO_2 molar content were investigated by cleaning gaseous toluene under UV irradiation. The gaseous toluene was placed in dark for 2 h without any light before photo-oxidation to achieve gas-solid adsorption equilibrium on the surface of fibrous catalysts. Then, the toluene in bottle was irradiated by a 300 W high pressure mercury lamp (λ = 365 nm, Yaming, Shanghai, China) while being stirred by a special magneton. The reacted gaseous samples were withdrawn at regular time intervals from 5 to 30 min by a 50 μL gastight pressure-locked precision analytical syringe (Gaoge, Shanghai, China) and measured with a gas chromatograph (Agilent 6890, USA) equipped with a flame ionization detector and an HP-5MS capillary column (0.25 mm i.d. × 30 m). A blank experiment without any catalyst under same conditions was also conducted as a comparison.

The degradation rate of gaseous toluene can be calculated by the following equation, where C_t is the concentration of toluene after several regular intervals of time (t), $C_{t=0}$ is the initial concentration of toluene.

$$\text{Degradation rate } \eta\,(\%) = \frac{C_{t=0} - C_t}{C_{t=0}} \times 100\%$$

For the purpose of investigation the intermediates on the surface of fibers, the used fibrous catalyst was recycled and dispersed in methanol (Fisher, HPLC grade), and was sonicated for 15 min, which was centrifuged for 15 min at 3000 rpm (Multifuge X1, Thermo Corporation, USA) and the upper solution was concentrated by rotary evaporation. The concentrated samples after methanol extraction were then tested through a gas chromatography and mass spectrometry (GC–MS, Aglient 6890, USA), in which HP-5MS capillary column was used with mass-to-charge of 45–260, and MS identification was based on the NIST 05 library with a fit higher than 90%.

3. Results and discussion

3.1. The microstructure of SiO_2 doped TiO_2 fibers

According to the TG curve of TiO_2 xerogel fibers (Fig. 1a), there are three weight loss steps and no further organics will be removed above 400 °C. And the total weight loss can reach 45.6%, which indicated that the organic component has been entirely decomposed. There was an obvious endothermic peak around 311 °C, indicating most of the organic components being decomposed. Based on the TG result, 400 °C was chosen as the optimum temperature to eliminate organic materials. The XRD patterns (Fig. 1b) revealed that anatase TiO_2 nanocrystals came into being after calcination at 300 °C. With calcination temperature reached 800 °C, the peaks became higher and higher, the intensity of anatase TiO_2 increased greatly, which is consistent with the results of FTIR, and much

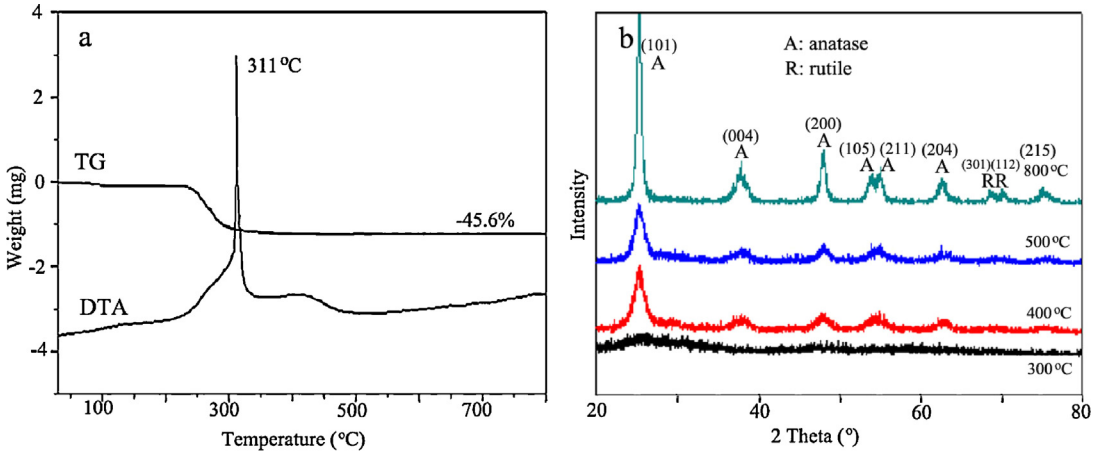

Fig. 1. (a) TG and DTA curve of 10% SiO_2 doped xerogel fibers and (b) XRD patterns of the nanostructured fibers at different sintered temperature.

bigger particle sizes can be found. In addition, there are little rutile phase TiO_2 came into being after the composite fibers were calcined at 800 °C. Because of lower concentration of doped SiO_2 and amorphous phase, the SiO_2 cannot be found in these XRD patterns.

The SEM images of the 10% SiO_2 doped TiO_2 nanostructured fibers are shown in Fig. 2a and b. After calcinations, it could be seen that the surface of xerogel fibers was much smoother and cleaner (Fig. 2a). After these xerogel fibers were calcined at different temperature in air, the SiO_2 doped TiO_2 fibers formed and their surface changed rougher and rougher, and many obvious defects can be found. And the diameters of SiO_2 doped TiO_2 fibers decreased from 30–300 nm to 20–200 nm, which is due to removal of the whole organics after calcination (Fig. 2b). The average diameter before and after calcinations is 100 nm and 80 nm, respectively. In addition, the average size nanofibers can be obtained through optimizing the electrospun process parameters, such as applied voltage, viscosity of gel precursor, ambient temperature, humidity, and so on [24–26]. As the smaller diameter of electrospun nanofibers, its active surface

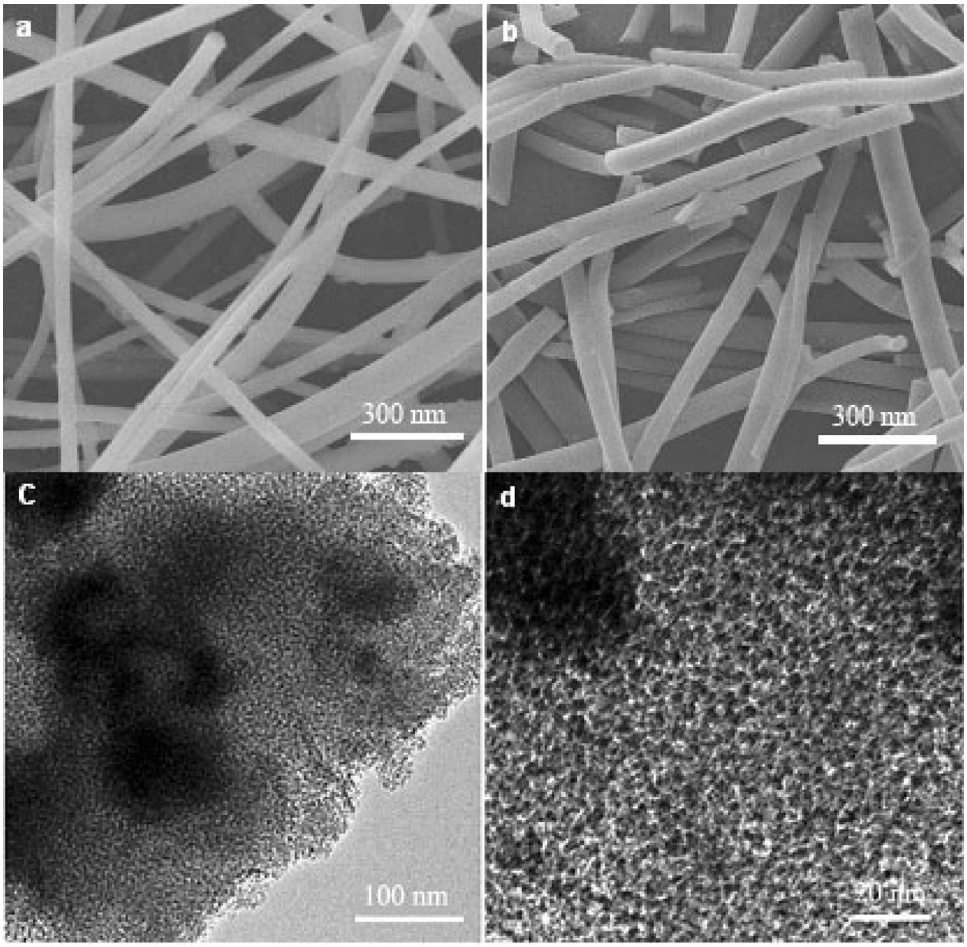

Fig. 2. SEM images of (a) xerogel fibers, (b) 10% SiO_2 doped TiO_2 fibers sintered at 400 °C, and (c, d) HRTEM images of the 10% SiO_2 doped TiO_2 fibers calcined at 400 °C in air.

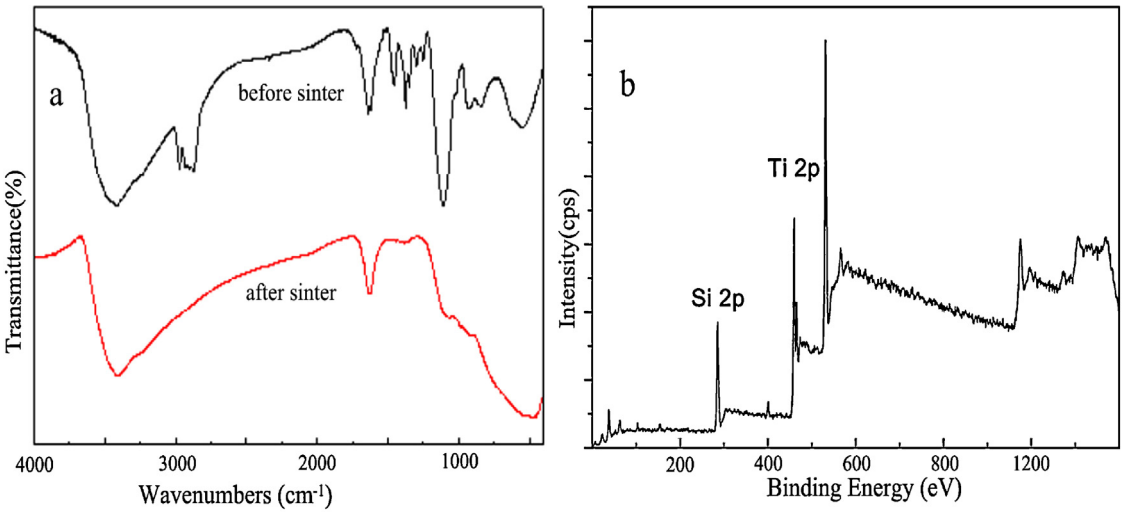

Fig. 3. (a) FTIR curves and (b) XPS spectrum of 10% SiO_2 doped TiO_2 nanofibers.

area became larger and larger, which is favor to improve degradation efficiency for cleaning toluene [27].

To further study the microstructure of fibers, the HRTEM images of 10% SiO_2 doped TiO_2 nanofibers was done (Fig. 2c and d). After calcination at 400 °C, anatase TiO_2 nanoparticles came into being with the average particle size of about 5 nm. Moreover, there are a good many of 3–4 nm worm-like pores in the fibers, these mesoporous channels will obviously increase fibrous catalyst's surface and their photocatalytic results [28,29]. By the way, these worm-like mesopores are beneficial for the connection of toluene molecules on the fibers' active points, increasing the toluene's cleaning efficiency, which has been verified in the following experiments.

The FTIR spectra of composite nanofibrous catalysts also verificated the above results (Fig. 3a). It can be found that there was a strong adsorption peak around 3400 cm^{-1}, which can be assigned to the hydroxyls from water, P123, Si–OH and Ti–OH. The weak peak at 1720 cm^{-1} also indicated the presence of water. While absorptions around 530 cm^{-1} appeared, it can be attributed to the Ti–O vibrations of TiO_2. When being calcinated at 400 °C, the peaks

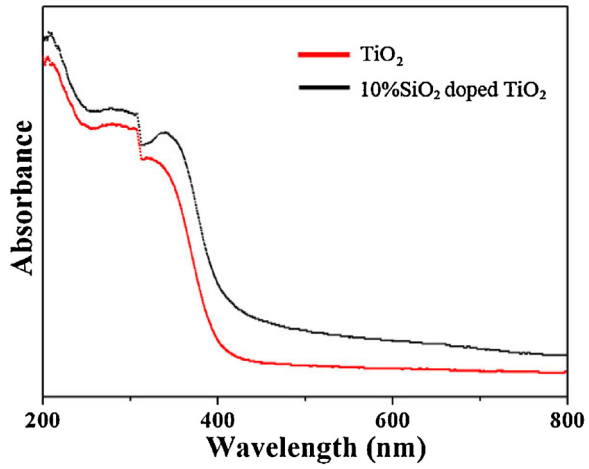

Fig. 4. UV–vis diffuse reflectance spectra of 10% SiO_2 doped TiO_2 and pure TiO_2.

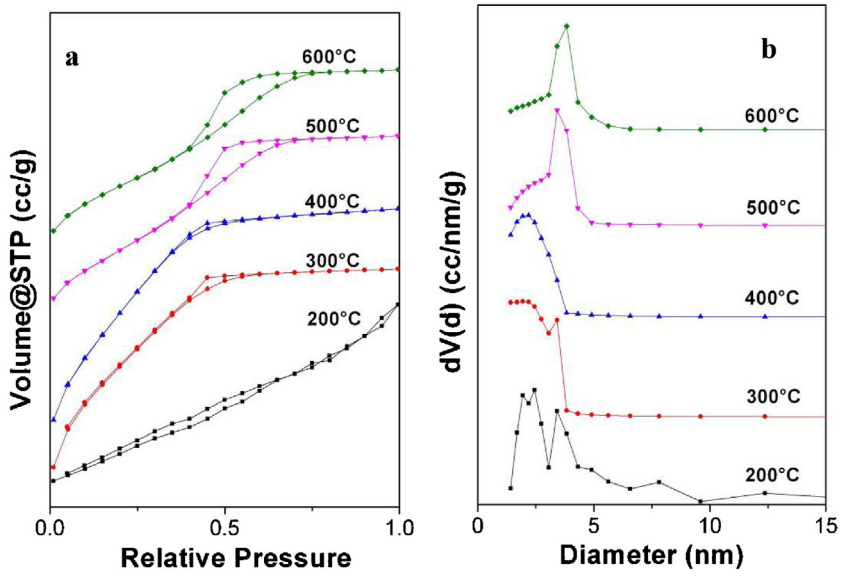

Fig. 5. (a) N_2 adsorption–desorption isotherm and (b) pore diameter distribution of calcined fibers at different sintered temperatures.

Table 1
The surface area, pore volume and pore diameters of fibers at different sintered temperature.

Temperature (°C)	Surface area (m^2/g)	Pore volume (cm^3/g)	Pore diameter (nm)
200	4.410	0.002	2.453
300	369.330	0.204	1.943
400	262.532	0.155	2.187
500	232.021	0.209	3.425
600	184.839	0.191	3.836

Table 2
The fiber's surface area, pore volume and pore diameter with different doped ratio.

Doped ratio of silica	Surface area (m^2/g)	Pore volume (cm^3/g)	Pore diameter (nm)
0%	100.133	0.189	3.821
1%	115.882	0.196	5.638
5%	194.693	0.248	4.905
10%	265.998	0.338	3.836
15%	272.798	0.236	3.420
20%	254.092	0.242	3.422

from 1520 to 1432 cm^{-1} almost disappeared, revealing the complete removal of P123, which is in accordance with those TG curves.

It was found that there were obvious characteristic peaks of silica, titanium and oxygen elements based on the XPS results of 10% SiO_2 doped TiO_2 fibers (Fig. 3b). From the spectrum, Ti-2p peak was located at 459.80 eV and the Si-2p peak was mainly located at 103.10 eV. The trace silica content has strongly coupled with titanium cell lattice based on following HRTEM results, which can decrease the light excitation level and decrease the difficulty to clean toluene.

In addition, UV–vis measurements have been done as shown in Fig. 4. It can be concluded that the 10% SiO_2 doped TiO_2 fibers have a broader absorption area, which show better degradation efficiency than pure TiO_2 fibrous catalysts without any silica. These UV–vis absorption data is consistent with photocatalytic results of cleaning toluene.

The N_2 adsorption–desorption isotherms of nanostructured fibers sintered at different heating temperatures were shown in Fig. 5, and the detailed data of pore size distribution, pore volume and surface area at different temperatures were listed in Table 1. After being sintered at 200 °C, the pore volume and surface area are very small and adsorption–desorption isotherm is almost close as type II, showing that the pore was still occupied with P123 molecular. At 300 °C, the adsorption capacity reached maximum and the catalyst adsorption isotherms has been converted into type IV curve, which also contains the H1 type hysteresis loop [30,31]. And the surface area of fibrous catalyst sintered at 400 °C, 500 °C and 600 °C is 263, 232 and 185 m^2/g respectively, which may greatly be attributed to the removal of P123 skeleton. Accordingly, the pore diameter and pore volume of the above fibers are 2.187, 3.425 and 3.836 nm, and 0.155, 0.209, 0.191 cm^3/g, these increasing trend is due to the full decomposition of P123, which is same with the TG and FTIR results.

As shown in Fig. 6, the adsorption–desorption curves of TiO_2 fibrous catalysts with different SiO_2 doped ratio are all type IV adsorption–desorption isotherms, which further demonstrate the presence of mesopores in these fibers [32]. The H1 type hysteresis loop indicated that the pore sizes were more uniform and the curves changed slightly in accordance with different SiO_2 doped ratios. With the increasing content of SiO_2 doped mole ratio, pore diameters became smaller and smaller.

It can be observed (Table 2) that the pore size distribution of pure TiO_2 fibers (without SiO_2) is from 3 nm to 7 nm, which is much broader compared to other fibers of different doped ratios. With the increasing doped content of SiO_2, pore diameter distribution became much narrower and uniform according to Fig. 6b. The surface area with the SiO_2 doped ratio at 1%, 5%, 10%, 15%, 20% was 100, 116, 195, 166, 273, 254 m^2/g and the corresponding pore diameter is 5.6, 4.9, 3.8, 3.4, 3.4 nm, which are obviously affected by the increasing SiO_2 content. Based on Table 2, the pore volume reached a highest value while SiO_2 doped ratio is 10%, which is 2863.18 ft^2/g of surface area and 0.338 cm^3/g of pore volume, respectively, which is favorable for more toluene molecules to contact with active points, further facilitating the interaction between hydroxyl radicals and toluene, and the degradation efficiency could be improved highly [33]. Although when the doped ratio is 15%, its surface area reached biggest, the fibrous catalysts' pore volume (272.798 m^2/g) and diameter (3.420 cm^3/g) is smaller than that one with 10% silica doped ratio.

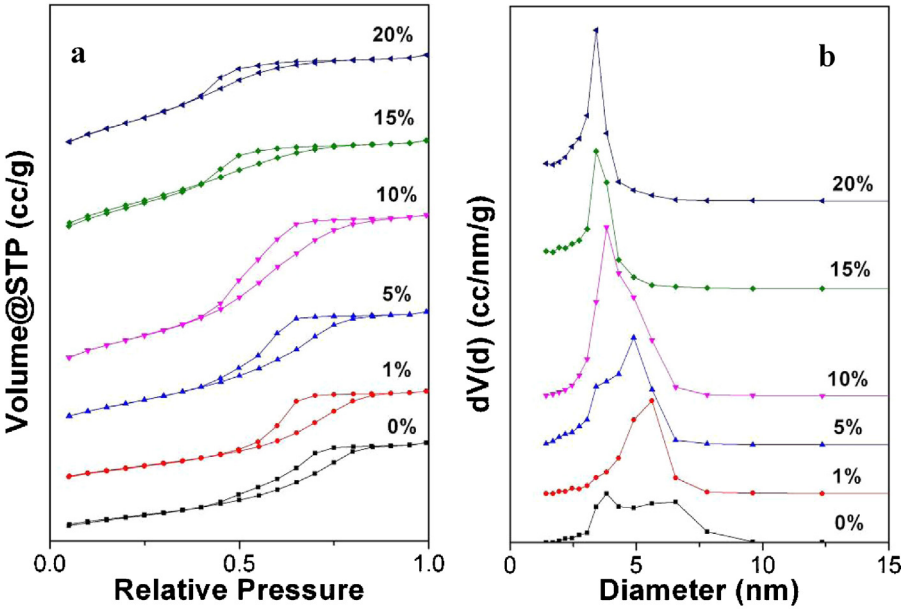

Fig. 6. (a) N_2 adsorption desorption isotherm and (b) pore diameter distribution of TiO_2 fibers with different SiO_2 doped ratio calcined at 400 °C.

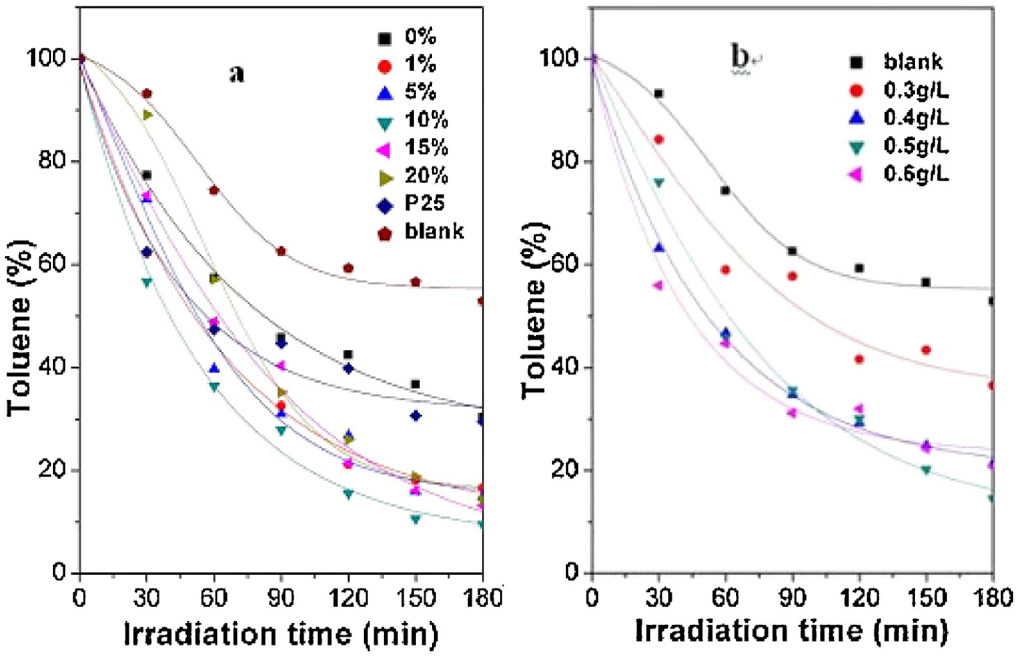

Fig. 7. The degradation efficiency of toluene by TiO_2 fibers with different doped SiO_2 (a) and different dosage (b).

Based on all the test results, 10% SiO_2 doped TiO_2 nanostructured fibrous catalyst calcined at 400 °C in air would have the highest effect while cleaning toluene in the following experiment, which has also been verified in the following photocatalytic experiment.

3.2. Photocatalytic activity

The effects of humidity and initial concentration of toluene on photocatalytic activity with 10% SiO_2 doped TiO_2 fibers are also tested. In our experiment, the initial toluene concentration was fixed as 7 mg/L, the humidity was 1.6 g/m^3 according to the preliminary experiments and former reports, a series of tests were done to remove toluene using TiO_2 fibrous catalysts with different SiO_2 doped ratio. As shown in Fig. 7a, the degradation efficiency of toluene was only 45.1% without any catalyst. However, the removal efficiency could reach 83.5%, 85.1%, 90.6%, 86.9% and 85.7%, with the doped ratio of SiO_2 is 1%, 5%, 10%, 15% and 20%, respectively. In comparison with pure TiO_2 fibers and Degussa P25, the removal efficiency was only 69.6% and 70.5%, which were also lower than TiO_2 fibers with different SiO_2 doped ratio. The 10% SiO_2 doped ratio has the highest degradation rate compared with all other catalysts or other SiO_2 doped ratio, which is mostly attributed to the lower light excited level through the couple effect between TiO_2 and optimal doped ratio SiO_2 [34].

Based on the experimental and characterization results, combined with a lot of published papers about SiO_2 doped TiO_2, the reasons for high degradation rate are the following:

In SiO_2 doped TiO_2 composites, the Si–O–Ti bond came into being, the surface area of composite fibers became larger and larger with the increase of doped silica ratio, as shown in Table 2. The larger surface area can result in more photocatalytic active points, which can increase its degradation rate.

On the other hand, according to XPS and FTIR results, the Ti–O–Si bond came into being and result in a lot of chemical defects on the surface of SiO_2 doped TiO_2 fibers, which can also increase the degradation rate. However, too high silica ratio will accelerate the recombination of electron and hole, which will decrease its degradation rate, such as the 15% silica doped TiO_2 [35,36].

The removal efficiency was also influenced by the different dose of catalysts (Fig. 7b). In this article, several different dose of 10% SiO_2 doped TiO_2 fibers (0.30 g/L, 0.40 g/L, 0.50 g/L, 0.60 g/L) were put into the reaction equipment to clean gaseous toluene while fixing other process parameters. It can be found that 0.5 g/L dose fibers showed the most excellent reduction rate. The cleaning rate of 0.6 g/L fibers was lower than 0.50 g/L, which may be due to the excessive fibrous catalyst would hider the light irradiation and reduce the practical active site [37–40].

3.3. Degradation mechanism of clean toluene

Every PCO reaction process of cleaning typical toluene has the corresponding intermediates, and most of them can maybe be toxic for human health. In the process of photocatalytic reaction, the generated intermediates were all strongly adsorbed on the surface of TiO_2 fibrous catalyst, which could hinder and reduce the quantities of electron–holes. On the other hand, the formation mechanism of extra byproducts can be controlled through the regulation of reaction parameters such as humidity. Therefore, it is necessary to identify the intermediates generated during the photocatalytic reaction and find its reaction mechanism [41].

The GC–MS test has been used to detect the adsorbed intermediates on the surface of fibrous composite catalysts. The

Table 3
The intermediates on the reacted catalysts.

Peak	RT	Area%	Species
1	6.097	0.50	Acetic acid, butyl ester
2	6.558	0.44	Acetic acid
3	8.514	0.56	Oxime-, methoxy-phenyl-
4	9.667	1.41	Benzaldehyde
5	9.842	0.61	1-Amino-2,6-dimethylpiperidine
6	10.532	0.13	Butanoic acid, hexyl ester
7	11.370	0.41	Benzyl Alcohol
8	11.531	0.87	Benzaldehyde, 2-hydroxy-
9	12.701	0.12	Isooctane, (ethenyloxy)-
10	12.947	2.80	Benzaldehyde dimethyl acetal
11	13.754	0.37	12-Azabicyclo[9.2.2]pentadecan-13-
12	14.234	8.13	Benzenecarboxylic acid

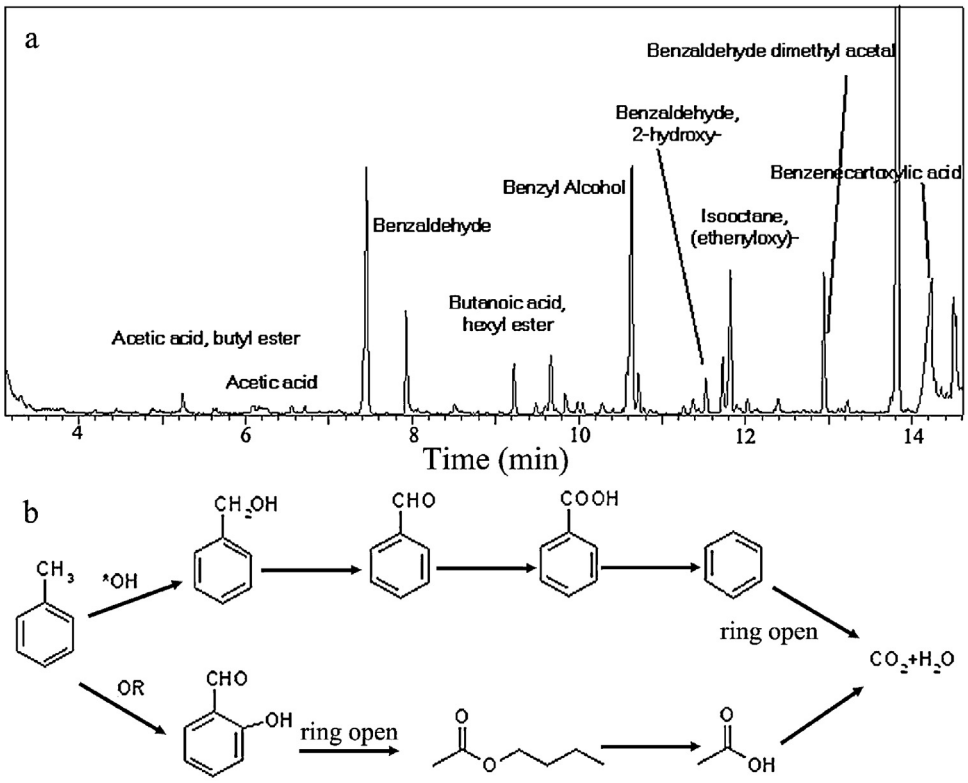

Fig. 8. (a) A representative GC–MS result and (b) degradation mechanism of toluene.

intermediates generated in the experiment are shown in Table 3. During the PCO process, UV irradiation is adequate to induce electron–hole pairs, most of which recombine and release the absorbed energy as light or heat, while a small percentage of these carriers transfer to the fibers' surface to start the catalytic cycle. Conduction band electrons can reduce electron acceptors like oxygen molecules or H^+, whereas valence band and electron–holes are oxidants that are able to attack donor species such as organic molecules or hydroxyl groups [8]. A series of complex intermediates have been found, such as benzaldehyde dimethyl acetal, benzyl alcohol, 1-amino-2,6-dimethylpiperidine, and so on (Table 3).

According to the identified intermediates, the degradation mechanisms are proposed in the following. As is shown in Fig. 8b, there were two different target sites on the toluene molecules UV light attacked firstly. One of the pathways was that a hydrogen atom was firstly extracted from the side chain of toluene and methyl groups of adsorbed toluene molecules, forming benzyl alcohol. The newly formed benzyl alcohol can be further oxidized to benzaldehyde and benzoic acid. On the other side, the hydroxyl radicals (·OH) maybe reacted directly on aromatic rings, yielding cresols and methyl was oxidized to aldehyde group immediately. Through the above reaction processes, the benzyl ring of toluene molecularls can be totally opened, and all intermediates can be entirely oxidized into CO_2 and H_2O, then toxic toluene could be removed completely.

4. Conclusions

Long mesoporous TiO_2 nanofibers with different SiO_2 doped ratio have been prepared by the sol–gel method combined with electrospinning technique. Based on experimental results, the mesoporous 10% SiO_2 doped TiO_2 fibrous catalysts calcined at 400 °C in air showed highest photocatalytic activity than a good many of different catalysts while cleaning indoor toluene. The degradation pathway was verified here and the formed complex hydroxyl derivatives were found and verified. In addition, these long composite fibers can be conveniently fixed and reclaimed, and they are good candidates for photocatalytic applications in air purification.

Acknowledgements

The authors gratefully acknowledge the financial support of National Natural Foundation of China (21377061, 21003094), Doctoral Program of Higher Education of China (20100032120066), Natural Science Foundation of Tianjin (12JCQNJC05800), Key Technologies R & D Program of Tianjin (13ZCZDSF00300) and the assistance of Dr. Haihua Xiao and Junjun Shan (University of Notre Dame) in manuscript preparation.

References

[1] T. Nguyen-Phan, M.B. Song, E.W. Shin, J. Hazard. Mater. 167 (2009) 75–81.
[2] J. Van Durme, J. Dewulf, W. Sysmans, C. Leys, H. Van Langenhove, Chemosphere 68 (2007) 1821–1829.
[3] C. He, L.L. Xu, L. Yue, Y.T. Chen, J.S. Chen, Z.P. Hao, Ind. Eng. Chem. Res. 51 (2012) 7211–7222.
[4] Y.C. Feng, L. Li, M. Ge, C.S. Guo, J.F. Wang, L. Liu, ACS Appl. Mater. Interfaces 2 (2010) 3134–3140.
[5] L.Y. Piao, Y.D. Li, J.L. Chen, L. Chang, J.Y.S. Lin, Catal. Today 74 (2002) 145–155.
[6] F. Dong, S. Guo, H.Q. Wang, X.F. Li, Z.B. Wu, J. Phys. Chem. C 115 (2011) 13285–13292.
[7] R.S. Walmsley, A.S. Ogunlaja, M.J. Coombes, J. Chidawanyika, C. Litwinski, N. Torto, T. Nyokong, Z.R. Tshentu, J. Mater. Chem. 22 (2012) 5792–5800.
[8] X.B. Li, L.L. Wang, X.H. Lu, J. Hazard. Mater. 177 (2010) 639–647.
[9] T. Wang, X. Jiang, Y.X. Wu, Ind. Eng. Chem. Res. 48 (2009) 6224–6228.
[10] S.W. Liu, J.G. Yu, M. Jaroniec, Chem. Mater. 23 (2011) 4085–4093.
[11] S.G. Kumar, L.G. Devi, J. Phys. Chem. A 115 (2011) 13211–13241.
[12] M.D. Hernandez-Alonso, F. Fresno, S. Suarez, J.M. Coronado, Energ. Environ. Sci. 2 (2009) 1231–1257.
[13] A.A. Ismail, S.A. Al-Sayari, D.W. Bahnemann, Catal. Today 209 (2013) 2–7.
[14] Y. Yokomizo, S. Krishnamurthy, P.V. Kamat, Catal. Today 199 (2013) 36–41.
[15] Y. Kuwahara, H. Yamashita, J. Mater. Chem. 21 (2011) 2407–2416.
[16] H. Li, S.Y. Gao, M.N. Cao, R. Cao, J. Colloid Inter. Sci. 394 (2013) 434–440.

[17] R. Didier, Catal. Today 122 (2007) 20–26.
[18] H.Q. Wang, Z.B. Wu, Y. Liu, J. Phys. Chem. C 113 (2009) 13317–13324.
[19] H. Ge, G.W. Chen, Q. Yuan, H.Q. Li, Chem. Eng. J. 127 (2007) 39–46.
[20] I.G. Loscertales, A. Barero, I. Guerrero, R. Cortijo, M. Marquez, A.M. Ganan-Calvo, Science 295 (2002) 1695–1698.
[21] E.T. Niles, J.D. Roehling, H. Yamagata, A.J. Wise, F.C. Spano, A.J. Moulé, J.K. Grey, J. Phys. Chem. Lett. 3 (2012) 259–263.
[22] M.X. Wang, Z.H. Huang, K. Shen, F.Y. Kang, K.M. Liang, Catal. Today 201 (2013) 109–114.
[23] C. Tang, C.D. Saquing, J.R. Harding, S.A. Khan, Macromolecules 43 (2009) 630–637.
[24] X.M. Xu, J.F. Zhang, Y.W. Fan, Biomacromolecules 11 (2010) 2283–2289.
[25] A. Sarafraz-Yazdi, H. Assadi, W.A. Wan Ibrahim, Ind. Eng. Chem. Res. 51 (2012) 3101–3107.
[26] L. Gottardo, S. Bernard, C. Gervais, K. Inzenhofer, G. Motz, M. Weinmann, C. Balan, P. Miele, J. Mater. Chem. 22 (2012) 7739–7750.
[27] S.H. Zhan, D.R. Chen, X.L. Jiao, C.H. Tao, J. Phys. Chem. B 110 (2006) 11199–11204.
[28] Q.F. Li, L.X. Zeng, J.C. Wang, D.P. Tang, B.Q. Liu, G.N. Chen, M.D. Wei, ACS Appl. Mater. Interfaces 4 (2011) 490–496.
[29] R. Ruiz-Rosas, J. Bedia, J.M. Rosas, M. Lallave, I.G. Loscertales, J. Rodríguez-Mirasol, T. Cordero, Catal. Today 187 (2012) 77–87.
[30] X.P. Wang, J.J. Yu, J. Chen, Z.P. Hao, Z.P. Xu, Environ. Sci. Technol. 42 (2008) 614–618.
[31] Z.X. Dong, Y.Q. Wu, R.L. Clark, Langmuir 27 (2011) 12417–12422.
[32] F. Bosc, D. Edwards, N. Keller, V. Keller, A. Ayral, Thin Solid Films 495 (2006) 272–279.
[33] S. Livraghi, K. Elghniji, A.M. Czoska, M.C. Paganini, E. Giamello, M. Ksibi, J. Photochem. Photobiol. A 205 (2009) 93–97.
[34] X.B. Chen, S.S. Mao, Chem. Rev. 107 (2007) 2891–2959.
[35] A.L. Linsebigler, G.Q. Lu, J.T. Yates, Chem. Rev. 95 (1995) 735–758.
[36] S.H. Xu, W.F. Shangguan, J. Yuan, M.X. Chen, J.W. Shi, Appl. Catal. B: Environ. 71 (2007) 177–184.
[37] Y.X. Li, G.F. Ma, S.Q. Peng, G.X. Lu, S.B. Li, Appl. Surf. Sci. 254 (2008) 6831–6836.
[38] J.F. Li, G.Z. Lu, Y.Q. Wang, Y. Guo, Y.L. Guo, J. Colloid Inter. Sci 377 (2012) 191–196.
[39] Z.B. Wu, F. Dong, Y. Liu, H.Q. Wang, Catal. Commun. 11 (2009) 82–86.
[40] S. Ardizzone, C.L. Bianchi, G. Cappelletti, A. Naldoni, C. Pirola, Environ. Sci. Technol. 42 (2008) 6671–6676.
[41] A.A. Ismail, S.A. Al-Sayari, D.W. Bahnemann, Catal. Today 208 (2013) 7–10.